



Published in final edited form as:

Cancer Res. 2008 August 1; 68(15): 6300–6305. doi:10.1158/0008-5472.CAN-08-0461.

Differential Cellular Internalization of Anti-CD19 and CD22 Immunotoxins Results in Different Cytotoxic Activity

Xing Du, Richard Beers, David J. FitzGerald^{*}, and Ira Pastan^{*}

Laboratory of Molecular Biology, Center for Cancer Research, National Cancer Institute, National Institutes of Health, Bethesda, Maryland

Abstract

B cell malignancies routinely express surface antigens CD19 and CD22. Immunotoxins against both antigens have been evaluated and the immunotoxins targeting CD22 are more active. To understand this disparity in cytotoxicity and guide the screening of therapeutic targets, we compared two immunotoxins, FMC63(Fv)-PE38 targeting CD19 and RFB4(Fv)-PE38 (BL22) targeting CD22. Six lymphoma cell lines have 4-9-fold more binding sites per cell for CD19 than for CD22, but BL22 is 4-140-fold more active than FMC63(Fv)-PE38, even though they have a similar cell binding affinity (K_d ~7 nM). In one hour, large amounts of BL22 are internalized (2-3-fold more than the number of CD22 molecules on the cell surface), while only 5.2-16.6% of surface bound FMC63(Fv)-PE38 is internalized. The intracellular reservoir of CD22 decreases greatly after immunotoxin internalization indicating it contributes to the uptake of BL22. Treatment of cells with cycloheximide does not reduce the internalization of BL22. Both internalized immunotoxins are located in the same vesicles. Our results show that the rapid internalization of large amounts of BL22 bound to CD22 makes CD22 a better therapeutic target than CD19 for immunotoxins and probably for other immunoconjugates that act inside cells.

Keywords

intracellular CD22; hematologic malignancies; antibody scFv; *Pseudomonas* exotoxin; cytotoxicity

Introduction

Cancer is the second leading cause of death in the United States. At the end of the nineteenth century, Paul Ehrlich proposed that it should be possible to develop drugs that would act as “magic bullets” and kill tumor cells with high specificity (1). The generation of monoclonal antibodies (mAbs) has begun to fulfill this goal, and they are widely used as diagnostic tools and therapeutic agents (2). Several mAbs have been approved for clinical use and are effective against some types of tumors (2). However, many cancers are resistant to treatment with mAbs. Thus, a great effort has been devoted to arming antibodies with cytotoxic drugs, radioisotopes, or toxins to enhance their therapeutic effects (3).

Immunotoxins (ITs), fusion proteins of antibody and toxin, derive their potency from the activity of the toxin and the number of molecules internalized. The specificity of the ITs result from the particular antibody to which they are attached. CD19 is a transmembrane glycoprotein that is widely expressed through normal B cell development and by many B lineage

Requests for reprints: Ira Pastan, Laboratory of Molecular Biology, National Cancer Institute, 37 Convent Dr., Rm. 5106, Bethesda, MD 20892-4264, Tel: (301) 496-4797; Fax: (301) 402-1344; e-mail: pastani@mail.nih.gov .

^{*}Co-senior authors

malignancies (4,5). Thus CD19 has been an attractive target for IT therapy. Several different anti-CD19 ITs have been constructed and shown to have *in vitro* activity (6-9), but in clinical trials these ITs have not shown durable responses (10-15). CD22 is another B cell surface glycoprotein expressed on normal and malignant B cells (16,17). ITs against CD22 showed potent *in vitro* activity (18,19) and have produced striking results in clinical trials for patients with drug resistant hairy cell leukemia (20,21). Given the abundant expression of CD19 and CD22, one possible explanation for better response when targeting CD22 is that the anti-CD19 ITs are not as potent for killing malignant cells as anti-CD22 ITs, a possibility which has been raised in comparison studies (9,22-24).

Using the anti-CD22 immunotoxin RFB4(Fv)-PE38 (BL22), our laboratory has shown that the IC₅₀ values for most cell lines range from 1-10 ng/ml (18,25), whereas a recent report with an anti-CD19 IT with a similar but not identical structure reported IC₅₀ values in the 100 ng/ml range (26). Because these immunotoxins are purified in different ways and contain slightly different forms of *Pseudomonas* exotoxin (PE), we prepared anti-CD19 and anti-CD22 CD22 ITs with similar methods, using the same PE38 form of the toxin so we could more directly compare them. To target CD19 we chose to use the Fv region of the FMC63 mAb because it is able to be internalized (27), and to target CD22 we used BL22 derived from the RFB4 mAb. We have compared the expression of CD19 and CD22 on various malignant B cell lines, the cytotoxic activities of the two ITs, and their rates and amounts of internalization. We also studied the contribution of intracellular CD22 to the rapid internalization of BL22 and determined intracellular localization of both ITs following their endocytosis. We found that the better cytotoxicity of BL22 results from its fast internalization rate, not from the different internalization pathway.

Materials and Methods

Cell lines

Human B cell lymphoma cell lines BL74, CA46, DOHH2, KEMI, Raji and Ramos were used in the current study. BL74 and KEMI were grown in IMDM with 10% FBS. CA46, DOHH2, Raji and Ramos were grown in RPMI 1640 medium with 10% FBS.

Preparation of immunotoxins

DNA sequences of the variable regions of immunoglobulin heavy chain (V_H) and light chain (V_L) for anti-CD19 mAb FMC63 (28) were retrieved from the European Bioinformatics Institute.¹ From the V_H and V_L sequences a single chain Fv (scFv) ORF was designed to contain an NdeI site at the 5' end followed by the V_H, a (GGGG) ×4 linker and a V_L with a HindIII restriction site at the 3' end. The gene was codon optimized for expression in *E. coli* and the DNA was synthesized by Blueheron Biotechnology Inc. (Bothell, WA) and inserted into pUC19. The scFv DNA was isolated from pUC19 by digestion with NdeI and HindIII and ligated into a T7 expression vector creating an in-frame fusion with PE38 (29). The plasmid sequence was verified by DNA sequencing.

The expression plasmid was transformed into *E. coli* strain BL21 (λDE3). One liter of culture was grown and induced at OD₆₀₀ of 2.0. The cell pellet from the culture was processed as previously described (29); 200 mg of inclusion body protein was refolded and purified (29). The final yield was 2.5%.

The anti-CD22 IT BL22 was reported previously (18). FMC63(Fv)-PE38 and BL22 were labeled with Alexa-488 or Alexa-594 according to the manufacturer's instructions (Invitrogen, Carlsbad, CA).

Antigens expression, cytotoxicity and affinity of immunotoxins

To determine the amount of CD19 or CD22 expressed on the surface of B cell lymphoma cell lines, we conducted two-step staining using the same second antibody to normalize the expression level. Cells (5×10^5) were incubated on ice with 10 $\mu\text{g/ml}$ (saturating concentration) anti-CD19 FMC63 mAb (Millipore, Billerica, MA) or anti-CD22 RFB4 mAb (purified from hybridoma supernatant in our laboratory), or an isotype control IgG1 (Sigma, St. Louis, MO). After washing, cells were incubated with goat anti-mouse PE conjugated F(ab) $'_2$ (BioSource, Camarillo, CA). Median fluorescence intensity (MFI) was analyzed with a FACSCalibur flow cytometer (BD Biosciences, San Jose, CA). QuantiBRITE PE Beads (BD Biosciences) were used as PE fluorescence standard to calculate the number of CD19 or CD22 sites per cell. For the following internalization and intracellular measurements, these surface antigen sites were represented by MFI of saturated binding on ice, and were used to calculate the number of internalized and intracellular molecules based on their respective MFIs.

Cytotoxicity of ITs was measured by a cell viability assay using WST-8 (Dojindo Molecular Technologies, Gaithersburg, MD) as reported previously (30). To evaluate the cell binding ability of ITs, different concentrations of Alexa-488 labeled FMC63(Fv)-PE38 and BL22 were incubated with DOHH2 cells on ice, and then analyzed with FACSCalibur. Binding saturation curves, nonlinear regression analysis and Scatchard plots were generated using Graph Pad Prism (Graph Pad Software, Inc., San Diego, CA).

Internalization of immunotoxins

For the time course of internalization, CA46 or DOHH2 cells were incubated with 100 nM or 10 nM Alexa-488 labeled FMC63(Fv)-PE38 or BL22 at 37°C for 0.25, 0.5, 1, 2, and 4 hr. To compare internalization between different cell lines, BL74, CA46, DOHH2, KEMI, Raji or Ramos cells were incubated with 100 nM or 10 nM Alexa-488 labeled FMC63(Fv)-PE38 or BL22 at 37°C for 1 hr. The cells were then stripped with glycine buffer (0.2 M, pH2.5, 1 mg/ml BSA) to remove surface bound ITs and analyzed with FACSCalibur. The surface bound amount at saturated concentration was conducted with 100 nM ITs on ice for 30 min. Alexa-488 labeled SS1P, an IT against mesothelin, was used as negative control (31).

To study the effect of protein synthesis inhibitor on BL22 internalization, DOHH2 cells were incubated with 20 $\mu\text{g/ml}$ cycloheximide at 37°C for 0, 2, or 4 hr. Then 100 nM Alexa-488 labeled BL22 was added and incubated at 37°C for an additional 30 or 60 min. Cells were stripped with glycine buffer and analyzed by flow cytometry.

To visualize the internalization by confocal fluorescence microscopy, D-polylysine treated cover glass slides (BD Biosciences) were placed into 24-well plates. CA46 cells (3×10^5) in 0.35 ml were added to each well. Cells were incubated at 37°C with 100 nM Alexa-488 labeled FMC63(Fv)-PE38 for 2 hr, and then 100 nM Alexa-594 labeled BL22 was added and incubated for another hr. Cells were concentrated onto slides by microcentrifuge (1200 rpm \times 5 min) and washed once with PBS once. ITs bound to the cell surface were stripped off by incubation in 0.35 ml glycine buffer for 10 min on ice followed by neutralization with 0.35 ml Tris (0.5 M pH 7.4) and a wash with PBS. Cells were then fixed in 3.7% formaldehyde for 1 hr on ice. Cells were incubated with DAPI for 5 min at room temperature and washed once. After air-drying, cover slides were mounted with ProLong Gold antifade reagent (Invitrogen). To monitor surface binding, cells were incubated with 100 nM Alexa-488 labeled FMC63(Fv)-PE38 or Alexa-594 labeled BL22 on ice for 1 hr and were processed without acid stripping. Slides were then analyzed with a Zeiss LSM 510 laser scanning microscopy (Carl Zeiss, Jena, Germany).

Intracellular CD22 measurement

To measure intracellular CD22, cells were incubated with 100 nM of RFB4 mAb on ice for 30 min to block surface CD22. Then cells were fixed and permeabilized with FIX&PERM cell permeabilization kit (Invitrogen). After incubation with 100 nM Alexa-488 labeled RFB4 mAb or 100 nM Alexa-488 labeled SS1P (as negative control) on ice for 30 min, cells were analyzed with flow cytometry. To measure surface expression of CD22, cells were incubated with 100 nM Alexa-488 labeled RFB4 mAb on ice for 30 min.

To detect change of intracellular CD22 levels after RFB4 internalization, cells were incubated at 37°C with or without RFB4 (100 nM) for 1 hr. The cell surface CD22 was then blocked by incubation with RFB4. Cells were then fixed, permeabilized, and stained with Alexa-488 labeled RFB4. For the internalization measurement, cells were incubated with 100 nM of Alexa-488 labeled RFB4 at 37°C for 1 hr. Then, the cells were stripped with glycine buffer to remove any RFB4-Alexa-488 remaining on the cell surface.

Results

CD19 and CD22 expression, and cytotoxicity of immunotoxins

The surface expression levels of CD19 and CD22 were examined on six B cell lymphoma lines: BL74, CA46, DOHH2, KEMI, Raji and Ramos. CD19 levels ranged from 210,000—578,000 sites per cell. In contrast, CD22 levels were 4-9-fold lower and ranged from 26,000—94,000 sites per cell (Table 1). Despite the fewer CD22 binding sites, BL22 was 25-140-fold more cytotoxic than the anti-CD19 IT FMC63(Fv)-PE38, except on KEMI cells where there was only a 4-fold increase in activity (Fig. 1A and Table 1). The IC₅₀s of BL22 ranged from 0.6-14 ng/ml, whereas the IC₅₀s of FMC63(Fv)-PE38 ranged from 50-550 ng/ml. The activities of both immunotoxins were specific for the Fv, because the IC₅₀ of SS1P, an IT with the same PE38 targeting mesothelin (which is not present on the cell lines tested) was >1000 ng/ml (data not shown).

One possible explanation for the difference in cytotoxic activity could be affinity. As shown in Fig. 1B, the affinities of the FMC63(Fv)-PE38 and BL22 are almost identical (K_d ~ 7 nM) when measured on DOHH2 cells, though the IC₅₀s of both ITs differ by over 100-fold. This finding indicates that cell binding affinity is not the reason for the low cytotoxic activity of the FMC63(Fv)-PE38.

Internalization rate for FMC63(Fv)-PE38 and BL22

In order to kill target cells, ITs must be internalized by endocytosis (32,33). To study internalization, both ITs were labeled with Alexa-488. Internalization was measured at two concentrations of each IT (100 nM and 10 nM) and was compared to the amount of IT bound to the cell surface at a saturated concentration. This value was set as 100%. As shown in Fig. 2, at 100 nM, 40,000 molecules of FMC63(Fv)-PE38 (11%) were internalized by CA46 cells after 15 min and 82,000 molecules (23%) after 4 hr. At 10 nM, 7,000 molecules of FMC63(Fv)-PE38 (2.0%) were internalized by CA46 cells after 15 min and 19,000 molecules (5.4%) after 4 hr. However, BL22 was internalized at a much faster rate. At 100 nM, 216,000 molecules of BL22 (230%) were internalized by CA46 cells after 15 min and 229,000 molecules (240%) after 4 hr. At 10 nM, 90,000 molecules of BL22 (96%) were internalized by CA46 cells after 15 min and 148,000 molecules (157%) after 4 hr. Similar results were observed using DOHH2 cells (Fig. 2).

The internalization of FMC63(Fv)-PE38 and BL22 at 100 nM and 10 nM were also measured on four other cell lines (Supplementary Table S1). At 100 nM, the amount of internalized BL22 is 2.8-4.6-fold greater than that of FMC63(Fv)-PE38. At 10 nM, there is relatively more BL22

internalized than FMC63(Fv)-PE38 (6.5-16.5-fold). In five of the six cell lines, we observed that the amount of BL22 internalized exceeded the amount bound on the cell surface by 2-3-fold, indicating that, except for the initial surface CD22, there might be additional CD22 molecules recruited to the cell surface over time, allowing a greater degree of BL22 internalization.

Intracellular CD22 contributes to the rapid internalization of BL22

To determine whether an intracellular reservoir of CD22 contributes to the fast internalization of BL22, we measured the amount of intracellular CD22. The intracellular CD22 molecules of BL74, CA46, DOHH2, KEMI, Raji and Ramos cells are 27,000, 98,000, 53,000, 13,000, 71,000, 50,000, respectively. The intracellular CD22 levels usually exceed surface CD22 levels (100%-140%), except in KEMI cells (39%). We monitored the intracellular CD22 level after incubation with or without RFB4 mAb at 37°C. BL22 was not used because we found that permeabilization buffer disrupted BL22/CD22 complexes and affected the measurement of intracellular CD22 (data not shown). To overcome this difficulty, we used mAb RFB4, which has a higher avidity than BL22 but contains the same Fv. As shown in Fig. 3A, intracellular CD22 of CA46 cells (MFI=360) increased slightly after incubation without RFB4 (MFI=506), but dropped quickly after incubation with RFB4 (MFI=102). Likewise, intracellular CD22 of DOHH2 cells (MFI=138) increased slightly after incubation without RFB4 (MFI=165), while it dropped quickly after incubation with RFB4 (MFI=31). We compared the amount of internalized RFB4, intracellular CD22, and intracellular CD22 after RFB4 internalization. For all the cell lines, detectable intracellular CD22 level decreased greatly after incubation with RFB4 (Table 2). It is worth noting that the internalized RFB4 almost equals the surface CD22 plus the decrease of intracellular CD22, which suggests that intracellular CD22 contributes to the quick internalization of BL22.

We also examined the contribution of newly synthesized CD22 to the amount of BL22 internalized. Cycloheximide (CHX) was used to inhibit protein synthesis to eliminate fresh CD22. As shown in Fig. 3B left panel, CHX treatment decreased surface bound BL22 from 46,000 (no CHX) to 35,000 and 29,000 (CHX 2 hr and CHX 4 hr). One possible explanation for this is that the surface CD22 is undergoing endocytosis constitutively (34). However, the internalization of BL22 only slightly decreased with CHX treatment (Fig. 3B, right panel). While this slight decrease in internalization may be due to decreased surface CD22, our results indicate that inhibiting protein synthesis does not have a significant impact on BL22 internalization.

Sub-cellular localization of FMC63(Fv)-PE38 and BL22

Although BL22 is internalized much faster and to a greater extent than FMC63(Fv)-PE38, a different endocytic pathway could also account for the difference in cytotoxicity. To examine this possibility, we used confocal fluorescence microscopy, because this method is widely used for sub-cellular co-localization of proteins (35). We found FMC63(Fv)-PE38 and BL22 were bound to cell surface on ice (Fig. 4A). While after incubation at 37°C, both ITs were internalized into cells (Fig. 4B). Strong co-localization was observed between the two ITs, suggesting that both ITs utilize a similar endocytic pathway, which may exclude different trafficking as one of the reasons for the lower cytotoxicity of FMC63(Fv)-PE38.

Discussion

Since ITs are developed for treatment of cancer, the factors influencing the cytotoxic efficacy are studied extensively (36-42). Those factors include type of antigen and target cell, antigen density, IT binding affinity, and IT binding epitope, which eventually determines the number of IT internalized or intracellular route after internalization.

Both CD19 and CD22 are well known B cell surface marker proteins, yet the anti-CD19 and anti-CD22 ITs exerted different efficacies (8,22-24). In the current study, we compared two ITs derived from PE38, FMC63(Fv)-PE38 and BL22 (against CD19 and CD22, respectively). Although the expression level of CD19 is greater than that of CD22, BL22 is 4-100-fold more cytotoxic than FMC63(Fv)-PE38. Our results suggest that the intracellular traffic route is not the reason for the lower activity of FMC63(Fv)-PE38 because both ITs share similar sub-cellular localization. Previous studies showed that immunotoxins targeting different epitopes on the same antigen can show different cytotoxic activities (30,40-42). Although we only examined one immunotoxin to CD19 in this study, we believe that epitope differences do not account for the low cytotoxic activity observed with FMC63(Fv)-PE38, because CD19 has been shown to possess a single dominant epitope or adjacent epitopes (43). To confirm this, we examined the ability of four different anti-CD19 antibodies (J25.C1, HD37, CB19 and HIB19) to compete with FMC63, and found all of them were able to completely block the binding of FMC63 to cells (data not shown).

The remarkable difference between the amounts of internalized ITs (Fig. 2 and Supplementary Table S1) indicates that a lower level of internalization is the likely reason for the weaker activity of FMC63(Fv)-PE38. The slow internalization of our anti-CD19 immunotoxin is consistent with the report of slow internalization of mAbs to CD19 by chronic lymphocytic leukemia cells (44). As shown in the internalization assay at 100 nM and 10 nM, a lower concentration of FMC63(Fv)-PE38 resulted in a disproportionately reduced level of internalization, as compared to BL22. It is imaginable that under even lower concentrations, such as 1 nM or 0.1 nM, the internalization difference between BL22 and FMC63(Fv)-PE38 will be even greater. This offers some explanation for the huge disparity between IC₅₀ of the two ITs, which are in the low nM range (1 nM IT=67 ng/ml).

The majority of BL22 internalization occurs within 15 min, which means that CD22 rapidly transports CD22/BL22 complex from the cell membrane. More importantly, CD22 can carry much more BL22 (>200-300%) than the amount initially bound on cell surface (100%). Nascent CD22 contributes little to this process because inhibition of CD22 synthesis by CHX did not significantly decrease the amount of internalized BL22, though treatment with CHX decreases cell surface CD22 level. One possible reason is that surface CD22 is continuously undergoing endocytosis (34). Without newly synthesized CD22 as a supplement, the cell surface CD22 level decreases over time. But the rate of spontaneous CD22 endocytosis is much slower than that of the CD22/BL22 complex.

CD22 expression has been reported on cell membrane and in cytoplasm (45-47). Our study showed that the intracellular CD22 reservoir contributes to BL22 internalization, suggesting that once surface CD22 and BL22 form a complex, the intracellular CD22 moves quickly to the cell surface and binds additional BL22. This is consistent with a similar report that cross-linking surface IgM or treatment with phosphotyrosine phosphatase inhibitor induces rapid movement of intracellular CD22 to the cell surface (48). Fig. 3B shows that the cell surface CD22 decreases continuously even with the existence of a large pool of intracellular CD22. This suggests that intracellular CD22 is sequestered inside the cell and only moves to cell surface after stimulation (either by mAb or IT). The underlying mechanism is not yet understood.

Whether CD22 is able to be recycled back to the cell surface is controversial. Shan and Press (34) suggested that the constitutive endocytosis of CD22 was terminal, leading to degradation of CD22 with a half-life of 8 hours without recycling to the cell surface in human B cell lines. Using CD22 transfected CHO cells, Tateno et al. showed that recycling of CD22 from the intracellular pool is possible, though the rate may be slow (49). Our data (Table 2) indicates that intracellular CD22 contributes to the transportation of BL22 and RFB4 mAb. KEMI cells

have the slowest internalization and the least intracellular CD22. It is unlikely that recycled CD22 is involved in the internalization, because the amount of internalized RFB4 is roughly equal to surface CD22 plus the decrease of intracellular CD22. Transferrin receptor (TfR) has been shown to be able to internalize 2-4 times the number of cell surface bound anti-TfR ITs into cells and these ITs showed potent cytotoxicity (37). TfR is known for its recycling ability and intracellular pool, thus may share a similar mechanism as intracellular CD22 utilized to internalize large amount of ITs.

Overall, our results showed that the rapid internalization of large amounts of BL22 makes CD22 a superior therapeutic target as compared to CD19. Intracellular CD22 plays an important role in this process and moves rapidly to the cell surface. To develop therapeutics agents targeting CD19 more efficiently, it is important to identify the sub-type of malignant cells with better capability to internalize anti-CD19 ITs. It was recently shown that CD21 expression decreases the internalization of anti-CD19 mAbs (50), thus the CD21⁻ and CD21^{low} malignant cells may be better targets for anti-CD19 therapy. Also the anti-CD19 mAb (CB19) is internalized more quickly than other anti-CD19 mAbs (50). Whether the 2-3-fold increased internalization can result in significant enhanced cytotoxicity will need further investigation.

Supplementary Material

Refer to Web version on PubMed Central for supplementary material.

Acknowledgements

We thank Drs. Robert Kreitman and Mitchell Ho for their helpful discussion, Dr. Xiu-Fen Liu and the NCI, CCR Confocal Microscopy Core Facility for assistance with confocal microscope, and the NIH Fellows Editorial Board and Anna Mazzuca for editorial assistance.

This research was supported by the Intramural Research Program of the National Institutes of Health, National Cancer Institute, Center for Cancer Research.

References

1. Schwartz RS. Paul Ehrlich's magic bullets. *N Engl J Med* 2004;350:1079–80. [PubMed: 15014180]
2. Adams GP, Weiner LM. Monoclonal antibody therapy of cancer. *Nat Biotechnol* 2005;23:1147–57. [PubMed: 16151408]
3. Wu AM, Senter PD. Arming antibodies: prospects and challenges for immunoconjugates. *Nat Biotechnol* 2005;23:1137–46. [PubMed: 16151407]
4. Nadler, LM.; Reinherz, EL.; Haynes, BF.; Bernstein, ID., editors. B-cell/leukemia panel workshop: summary and comments. Springer-Verlag; New York: 1986. Leukocyte typing II; p. 3
5. Sato, S.; Tedder, TF.; Kishimoto, T., et al., editors. White cell differentiation antigens. 6th edition. Garland Publishing; New York: 1999. BC3, CD19 workshop panel report. leukocyte typing VI; p. 133-4.
6. Ghetie MA, Picker LJ, Richardson JA, Tucker K, Uhr JW, Vitetta ES. Anti-CD19 inhibits the growth of human B-cell tumor lines in vitro and of Daudi cells in SCID mice by inducing cell cycle arrest. *Blood* 1994;83:1329–36. [PubMed: 7509655]
7. Bregni M, Siena S, Formosa A, et al. B-cell restricted saporin immunotoxins: activity against B-cell lines and chronic lymphocytic leukemia cells. *Blood* 1989;73:753–62. [PubMed: 2465042]
8. Ghetie MA, May RD, Till M, et al. Evaluation of ricin A chain-containing immunotoxins directed against CD19 and CD22 antigens on normal and malignant human B-cells as potential reagents for in vivo therapy. *Cancer Res* 1988;48:2610–7. [PubMed: 2451562]
9. Uckun FM, Ramakrishnan S, Houston LL. Increased efficiency of selective elimination of leukemic cells by combination of a stable derivative of cyclophosphamide and a human B-cell specific immunotoxin containing pokeweed antiviral protein. *Cancer Res* 1985;45:69–75. [PubMed: 3871174]

10. Tsimberidou AM, Giles FJ, Kantarjian HM, Keating MJ, O'Brien SM. Anti-B4 blocked ricin post chemotherapy in patients with chronic lymphocytic leukemia--long-term follow-up of a monoclonal antibody-based approach to residual disease. *Leuk Lymphoma* 2003;44:1719–25. [PubMed: 14692524]
11. Szatrowski TP, Dodge RK, Reynolds C, et al. Lineage specific treatment of adult patients with acute lymphoblastic leukemia in first remission with anti-B4-blocked ricin or high-dose cytarabine: cancer and leukemia group B study 9311. *Cancer* 2003;97:1471–80. [PubMed: 12627512]
12. Multani PS, O'Day S, Nadler LM, et al. Phase II clinical trial of bolus infusion anti-B4 blocked ricin immunoconjugate in patients with relapsed B-cell non-Hodgkin's lymphoma. *Clin Cancer Res* 1998;4:2599–604. [PubMed: 9829722]
13. Grossbard ML, Fidias P, Kinsella J, et al. Anti-B4-blocked ricin: a phase II trial of 7 day continuous infusion in patients with multiple myeloma. *Br J Haematol* 1998;102:509–15. [PubMed: 9695966]
14. Grossbard ML, Lambert JM, Goldmacher VS, et al. Anti-B4-blocked ricin: a phase I trial of 7-day continuous infusion in patients with B-cell neoplasms. *J Clin Oncol* 1993;11:726–37. [PubMed: 7683045]
15. Grossbard ML, Freedman AS, Ritz J, et al. Serotherapy of B-cell neoplasms with anti-B4-blocked ricin: a phase I trial of daily bolus infusion. *Blood* 1992;79:576–85. [PubMed: 1370636]
16. Mason DY, Stein H, Gerdes J, et al. Value of monoclonal anti-CD22 (p135) antibodies for the detection of normal and neoplastic B lymphoid cells. *Blood* 1987;69:836–40. [PubMed: 3101766]
17. Tedder TF, Tuscano J, Sato S, Kehrl JH. CD22, a B lymphocyte-specific adhesion molecule that regulates antigen receptor signaling. *Annu Rev Immunol* 1997;15:481–504. [PubMed: 9143697]
18. Mansfield E, Amlot P, Pastan I, FitzGerald DJ. Recombinant RFB4 immunotoxins exhibit potent cytotoxic activity for CD22-bearing cells and tumors. *Blood* 1997;90:2020–6. [PubMed: 9292538]
19. Ghetie MA, Richardson J, Tucker T, Jones D, Uhr JW, Vitetta ES. Antitumor activity of Fab' and IgG-anti-CD22 immunotoxins in disseminated human B lymphoma grown in mice with severe combined immunodeficiency disease: effect on tumor cells in extranodal sites. *Cancer Res* 1991;51:5876–80. [PubMed: 1933855]
20. Kreitman RJ, Squires DR, Stetler-Stevenson M, et al. Phase I trial of recombinant immunotoxin RFB4 (dsFv)-PE38 (BL22) in patients with B-cell malignancies. *J Clin Oncol* 2005;23:6719–29. [PubMed: 16061911]
21. Kreitman RJ, Wilson WH, Bergeron K, et al. Efficacy of the anti-CD22 recombinant immunotoxin BL22 in chemotherapy-resistant hairy-cell leukemia. *N Engl J Med* 2001;345:241–7. [PubMed: 11474661]
22. Bonardi MA, French RR, Amlot P, Gromo G, Modena D, Glennie MJ. Delivery of saporin to human B-cell lymphoma using bispecific antibody: targeting via CD22 but not CD19, CD37, or immunoglobulin results in efficient killing. *Cancer Res* 1993;53:3015–21. [PubMed: 7686448]
23. Ghetie M, Tucker K, Richardson J, Uhr JW, Vitetta ES. The antitumor activity of an anti-CD22 immunotoxin in SCID mice with disseminated Daudi lymphoma is enhanced by either an anti-CD19 antibody or an anti-CD19 immunotoxin. *Blood* 1992;80:2315–20. [PubMed: 1384801]
24. Kiesel S, Pezzutto A, Haas R, Moldenhauer G, Dorken B. Functional evaluation of CD19- and CD22-negative variants of B-lymphoid cell lines. *Immunology* 1988;64:445–50. [PubMed: 3261711]
25. Salvatore G, Beers R, Margulies I, Kreitman RJ, Pastan I. Improved cytotoxic activity toward cell lines and fresh leukemia cells of a mutant anti-CD22 immunotoxin obtained by antibody phage display. *Clin Cancer Res* 2002;8:995–1002. [PubMed: 11948105]
26. Schwemmlin M, Stieglmaier J, Kellner C, et al. A CD19-specific single-chain immunotoxin mediates potent apoptosis of B-lineage leukemic cells. *Leukemia* 2007;21:1405–12. [PubMed: 17495978]
27. Sapra P, Allen TM. Internalizing antibodies are necessary for improved therapeutic efficacy of antibody-targeted liposomal drugs. *Cancer Res* 2002;62:7190–4. [PubMed: 12499256]
28. Nicholson IC, Lenton KA, Little DJ, et al. Construction and characterisation of a functional CD19 specific single chain Fv fragment for immunotherapy of B lineage leukaemia and lymphoma. *Mol Immunol* 1997;34:1157–65. [PubMed: 9566763]
29. Pastan I, Beers R, Bera TK. Recombinant immunotoxins in the treatment of cancer. *Methods Mol Biol* 2004;248:503–18. [PubMed: 14970517]

30. Du X, Nagata S, Ise T, Stetler-Stevenson M, Pastan I. FCRL1 on chronic lymphocytic leukemia, hairy cell leukemia and B-cell non-Hodgkin's lymphoma as a target of immunotoxins. *Blood* 2008;111:338–43. [PubMed: 17895404]
31. Hassan R, Bera T, Pastan I. Mesothelin: a new target for immunotherapy. *Clin Cancer Res* 2004;10:3937–42. [PubMed: 15217923]
32. Pastan I, Hassan R, Fitzgerald DJ, Kreitman RJ. Immunotoxin therapy of cancer. *Nat Rev Cancer* 2006;6:559–65. [PubMed: 16794638]
33. Pastan I, Hassan R, Fitzgerald DJ, Kreitman RJ. Immunotoxin treatment of cancer. *Annu Rev Med* 2007;58:221–37. [PubMed: 17059365]
34. Shan D, Press OW. Constitutive endocytosis and degradation of CD22 by human B cells. *J Immunol* 1995;154:4466–75. [PubMed: 7722303]
35. Ojcius DM, Niedergang F, Subtil A, Hellio R, Dautry-Varsat A. Immunology and the confocal microscope. *Res Immunol* 1996;147:175–88. [PubMed: 8817746]
36. Preijers FW, Tax WJ, De Witte T, et al. Relationship between internalization and cytotoxicity of ricin A-chain immunotoxins. *Br J Haematol* 1988;70:289–94. [PubMed: 3264717]
37. Goldmacher VS, Scott CF, Lambert JM, et al. Cytotoxicity of gelonin and its conjugates with antibodies is determined by the extent of their endocytosis. *J Cell Physiol* 1989;141:222–34. [PubMed: 2528553]
38. Youle RJ, Neville DM Jr. Kinetics of protein synthesis inactivation by ricin-anti Thy 1.1 monoclonal antibody hybrids. Role of the ricin B subunit demonstrated by reconstitution. *J Biol Chem* 1982;257:1598–601. [PubMed: 6120167]
39. Ramakrishnan S, Houston LL. Comparison of the selective cytotoxic effects of immunotoxins containing ricin A chain or pokeweed antiviral protein and anti Thy 1.1 monoclonal antibodies. *Cancer Res* 1984;44:201–8. [PubMed: 6140077]
40. Press OW, Martin PJ, Thorpe PE, Vitetta ES. Ricin A-chain containing immunotoxins directed against different epitopes on the CD2 molecule differ in their ability to kill normal and malignant T cells. *J Immunol* 1988;141:4410–7. [PubMed: 2461993]
41. Luo Y, Seon BK. Marked difference in the in vivo antitumor efficacy between two immunotoxins targeted to different epitopes of common acute lymphoblastic leukemia antigen (CD10). Mechanisms involved in the differential activities of immunotoxins. *J Immunol* 1990;145:1974–82. [PubMed: 1697314]
42. May RD, Wheeler HT, Finkelman FD, Uhr JW, Vitetta ES. Intracellular routing rather than cross-linking or rate of internalization determines the potency of immunotoxins directed against different epitopes of sIgD on murine B cells. *Cell Immunol* 1991;135:490–500. [PubMed: 1709828]
43. Zhou, L.-J.; Tedder, TF. CD19 Workshop panel report. In: Schlossman, SF.; Boumsell, L.; Gilks, W.; Harlan, JM., et al., editors. *Leukocyte Typing V*. Oxford University Press; Boston: 1995. p. 507-9.
44. Sieber T, Schoeler D, Ringel F, Pascu M, Schriever F. Selective internalization of monoclonal antibodies by B-cell chronic lymphocytic leukaemia cells. *Br J Haematol* 2003;121:458–61. [PubMed: 12716368]
45. Janossy G, Coustan-Smith E, Campana D. The reliability of cytoplasmic CD3 and CD22 antigen expression in the immunodiagnosis of acute leukemia: a study of 500 cases. *Leukemia* 1989;3:170–81. [PubMed: 2465463]
46. Boue DR, LeBien TW. Expression and structure of CD22 in acute leukemia. *Blood* 1988;71:1480–6. [PubMed: 3258772]
47. Pezzutto A, Rabinovitch PS, Dorken B, Moldenhauer G, Clark EA. Role of the CD22 human B cell antigen in B cell triggering by anti-immunoglobulin. *J Immunol* 1988;140:1791–5. [PubMed: 3257985]
48. Sherbina NV, Linsley PS, Myrdal S, et al. Intracellular CD22 rapidly moves to the cell surface in a tyrosine kinase dependent manner following antigen receptor stimulation. *J Immunol* 1996;157:4390–8. [PubMed: 8906814]
49. Tateno H, Li H, Schur MJ, et al. Distinct endocytic mechanisms of CD22 (Siglec-2) and Siglec-F reflect roles in cell signaling and innate immunity. *Mol Cell Biol* 2007;27:5699–710. [PubMed: 17562860]

50. Ingle GS, Chan P, Elliott JM, et al. High CD21 expression inhibits internalization of anti-CD19 antibodies and cytotoxicity of an anti-CD19-drug conjugate. *Br J Haematol* 2008;140:46–58. [PubMed: 17991300]

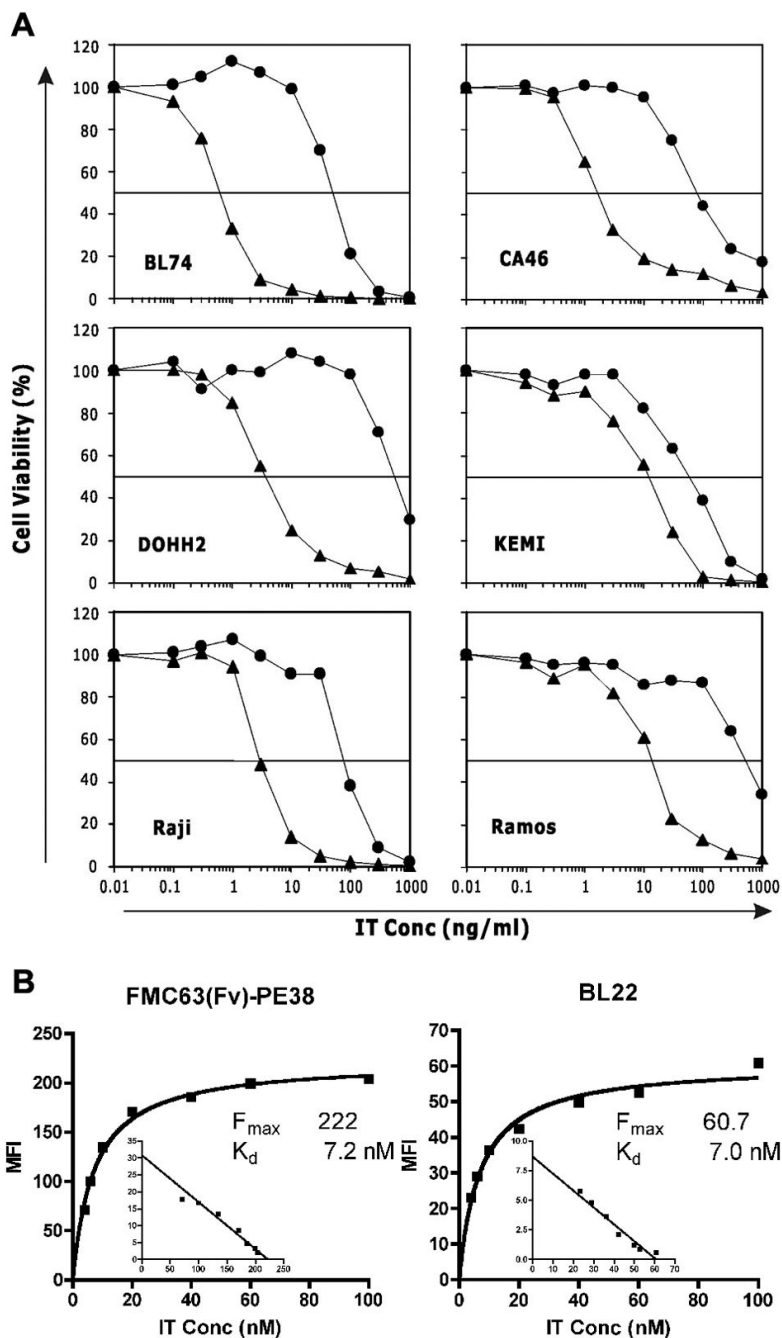


Figure 1. The cytotoxicity and affinity of FMC63(Fv)-PE38 and BL22. **A.** Cytotoxicity of ITs. Different concentrations of FMC63(Fv)-PE38 (●) or BL22 (▲) were incubated with cells. The IC₅₀ was determined by cell viability. Assays were performed in triplicate and SD was <10%. **B.** Cell binding affinity of ITs. DOHH2 cells were incubated with different concentrations of Alexa-488 labeled ITs and analyzed by flow cytometry. Two experiments showed concordant results.

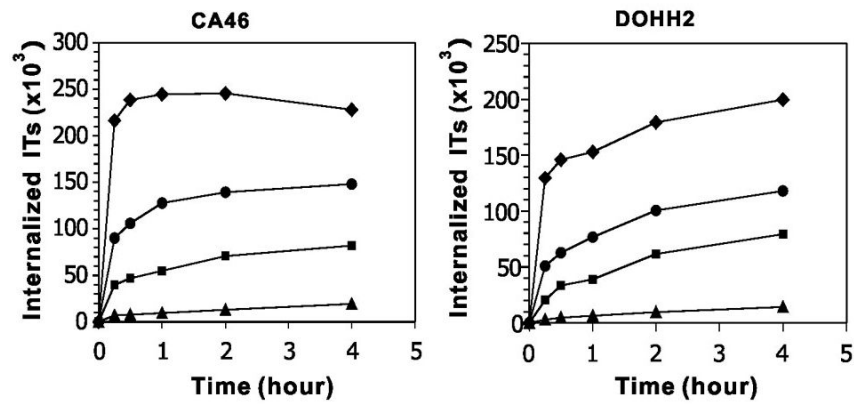


Figure 2. Time course of immunotoxin internalization. Cells were incubated with 100 nM or 10 nM Alexa-488 labeled BL22 or FMC63(Fv)-PE38 at 37°C for different times. (◆), 100 nM BL22; (●), 10 nM BL22; (■), 100 nM FMC63(Fv)-PE38; (▲) 10 nM FMC63(Fv)-PE38. The experiment shown is a representative of four similar experiments.

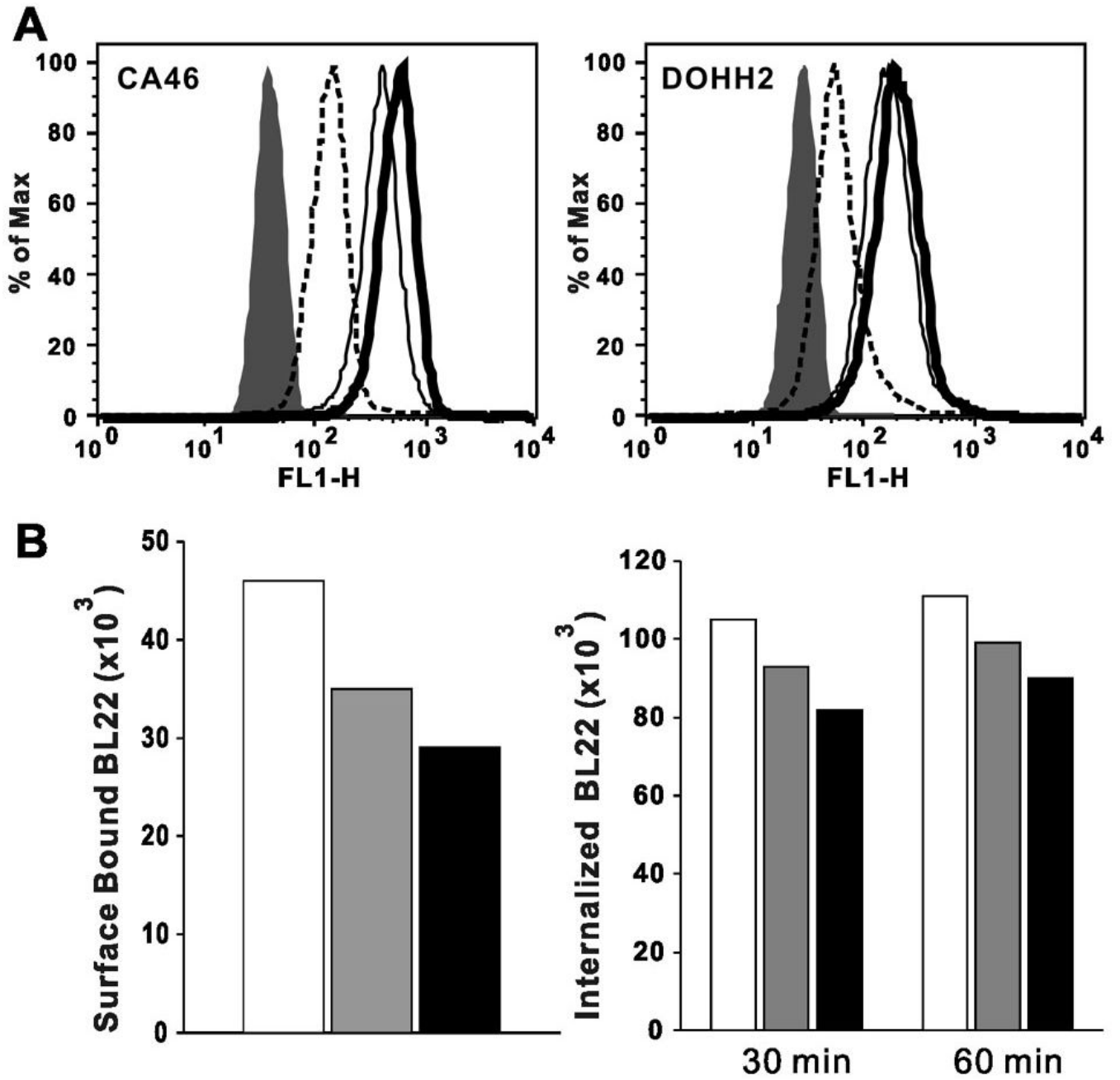


Figure 3.

The effects of intracellular CD22 and newly synthesized CD22 on internalization. **A.** Change of intracellular CD22 level after internalization of RFB4. CA46 and DOHH2 cells were incubated on ice, at 37°C with or without RFB4 (100 nM) for 1 hr, and then the intracellular CD22 was measured by Alexa-488 labeled RFB4 and analyzed by flow cytometry. Filled region, SS1P (negative control); dashed line (intracellular CD22 with RFB4); thin line (intracellular CD22); thick line (intracellular CD22 without RFB4). Three experiments showed concordant results. **B.** BL22 internalization after CHX treatment. Left panel, cell surface bound BL22. DOHH2 cells were treated by 20 µg/ml of CHX at 37°C for 2 and 4 hr. Then non-treated and treated cells were incubated with 100 nM Alexa-488 labeled BL22 on ice. Right panel,

internalization of BL22. CHX treated or non-treated cells were incubated with Alexa-488 labeled BL22 at 37°C for 30 and 60 min for internalization. White column, No CHX; Gray column, CHX 2 hr; Black column, CHX 4 hr. Three experiments showed concordant results.

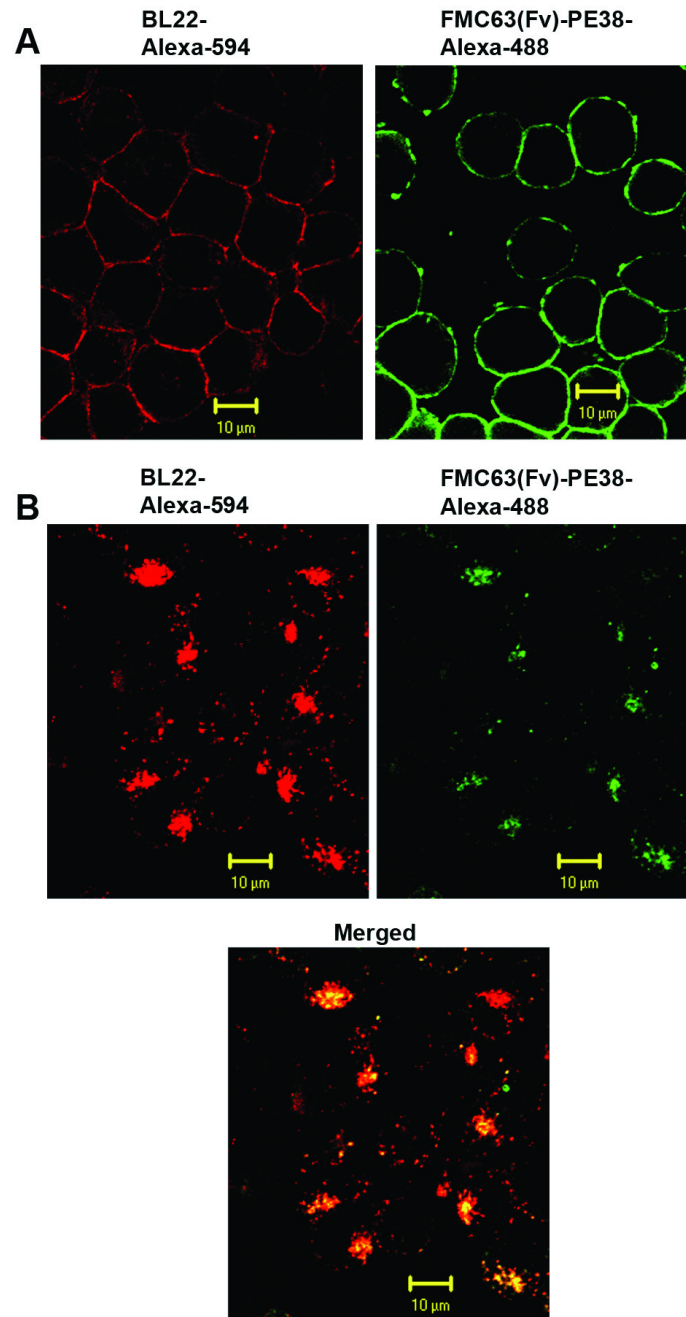


Figure 4. Sub-cellular localization of FMC63(Fv)-PE38 and BL22. **A.** Cell surface binding of ITs. CA46 cells were incubated with Alexa-488 (green) labeled FMC63(Fv)-PE38 or Alexa-594 (red) labeled BL22 on ice. **B.** Internalization of ITs. CA46 cells were incubated with Alexa-488 labeled FMC63(Fv)-PE38 at 37°C for 2 hr, then Alexa-594 labeled BL22 was added and incubated at 37°C for 1 hr. The surface bound immunoxins were stripped by glycine buffer.

Table 1
Expression levels of CD19 and CD22 and the cytotoxicity of immunotoxins

	CD19			CD22		
	MFI [*]	Sites/cell	IC ₅₀ [†]	MFI	Sites/cell	IC ₅₀
BL74	720	236,000	50	68	26,000	0.6
CA46	1085	354,000	80	280	94,000	1.4
DOHH2	734	241,000	550	130	46,000	4
KEMI	640	210,000	55	90	33,000	13
Raii	1780	578,000	73	180	62,000	3
Ramos	676	222,000	500	98	35,000	14

* Flow cytometry was conducted with two-step staining. First FMC63 mAb or RFB4 mAb, then goat anti-mouse PE conjugated F(ab)².

[†] Cytotoxicity was determined by WST-8 cell viability assay.

Table 2 Relationship between internalization of RFB4 and intracellular CD22 change

	CD22 [*]	RFB4 [†]	CD22 [†]	CD22 (with RFB4) [†]	CD22 [†]	CD22+CD22 [†]
BL74	26,000	44,000	27,000	10,000	17,000	43,000
CA46	94,000	165,000	94,000	26,000	68,000	162,000
DOHH2	46,000	113,000	53,000	12,000	41,000	87,000
Ramos	35,000	75,000	51,000	14,000	37,000	72,000

* CD22, cell surface CD22.

[†] RFB4, internalized RFB4.

[†] CD22, intracellular CD22.

[#] CD22, the decrease of intracellular CD22 = $\dot{CD22} - \dot{CD22}$ (with RFB4).